



# LUND UNIVERSITY

## Self-aligned, gate-last process for vertical InAs nanowire MOSFETs on Si

Berg, Martin; Persson, Karl-Magnus; Kilpi, Olli-Pekka; Svensson, Johannes; Lind, Erik; Wernersson, Lars-Erik

*Published in:*

Technical Digest - International Electron Devices Meeting, IEDM

*DOI:*

[10.1109/IEDM.2015.7409806](https://doi.org/10.1109/IEDM.2015.7409806)

2016

[Link to publication](#)

*Citation for published version (APA):*

Berg, M., Persson, K.-M., Kilpi, O.-P., Svensson, J., Lind, E., & Wernersson, L.-E. (2016). Self-aligned, gate-last process for vertical InAs nanowire MOSFETs on Si. In *Technical Digest - International Electron Devices Meeting, IEDM* (Vol. 2016-February). Article 7409806 IEEE - Institute of Electrical and Electronics Engineers Inc.. <https://doi.org/10.1109/IEDM.2015.7409806>

*Total number of authors:*

6

### General rights

Unless other specific re-use rights are stated the following general rights apply:

Copyright and moral rights for the publications made accessible in the public portal are retained by the authors and/or other copyright owners and it is a condition of accessing publications that users recognise and abide by the legal requirements associated with these rights.

- Users may download and print one copy of any publication from the public portal for the purpose of private study or research.
- You may not further distribute the material or use it for any profit-making activity or commercial gain
- You may freely distribute the URL identifying the publication in the public portal

Read more about Creative commons licenses: <https://creativecommons.org/licenses/>

### Take down policy

If you believe that this document breaches copyright please contact us providing details, and we will remove access to the work immediately and investigate your claim.

LUND UNIVERSITY

PO Box 117  
221 00 Lund  
+46 46-222 00 00

# Self-Aligned, Gate-Last Process for Vertical InAs Nanowire MOSFETs on Si

Martin Berg, Karl-Magnus Persson, Olli-Pekka Kilpi, Johannes Svensson,  
Erik Lind, and Lars-Erik Wernersson

Department of Electrical and Information Technology, Lund University, Box 118, Lund, Sweden  
E-mail: martin.berg@eit.lth.se Phone: +46462220000

## I. ABSTRACT

In this work, we present a novel self-aligned gate-last fabrication process for vertical nanowire metal-oxide-semiconductor field-effect transistors. The fabrication method allows for exposure dose-defined gate lengths and a local diameter reduction of the intrinsic channel segment, while maintaining thicker highly doped access regions. Using this process, InAs nanowire transistors combining good on- and off-performance are fabricated demonstrating  $Q = g_{m,max}/SS = 8.2$ , which is higher than any previously reported vertical nanowire MOSFET.

## II. INTRODUCTION

III-V compound semiconductors on Si substrates are expected to appear in commercial complementary metal-oxide-semiconductor (CMOS) implementations within a couple of years [1], taking advantage of the excellent transport properties of these semiconductors to reach faster and more energy-efficient circuits. One way to ensure high-quality materials for such highly lattice-mismatched integration, is through the use of a nanowire geometry [2]. Vertical nanowire MOSFETs allow for small footprints, as the channel and metal contact lengths are decoupled. It has been suggested that such integration can outperform lateral devices at highly scaled technology nodes [3], [4]. Furthermore, the geometry simplifies the fabrication of a gate-all-around transistor, which ensures good electrostatic control of the transistor channel. Reducing the nanowire diameter further improves electrostatics, but can also increase the series resistance from the ungated regions as well as increasing the metal-semiconductor contact resistance. One way of reducing these resistances is through high doping in the contact regions, which could be accomplished during nanowire growth. However, high-precision doping control of the nanowire core along the axial direction has proven very challenging [5], resulting in imprecise alignment of the electrodes and separation layers.

To address these issues, we have developed a self-aligned, gate-last process, allowing for local reduction of the nanowire diameter in the channel region using digital etching. InAs nanowires with a doped outer shell around an undoped core are used to implement transistors with a thin intrinsic channel and thicker doped contact regions. Furthermore, the process allows for the fabrication of MOSFETs with varying gate lengths,  $L_G$ , on the same sample. Using the described methods, the best combined performance of transconductance and subthreshold slope for any vertical nanowire MOSFET is demonstrated.

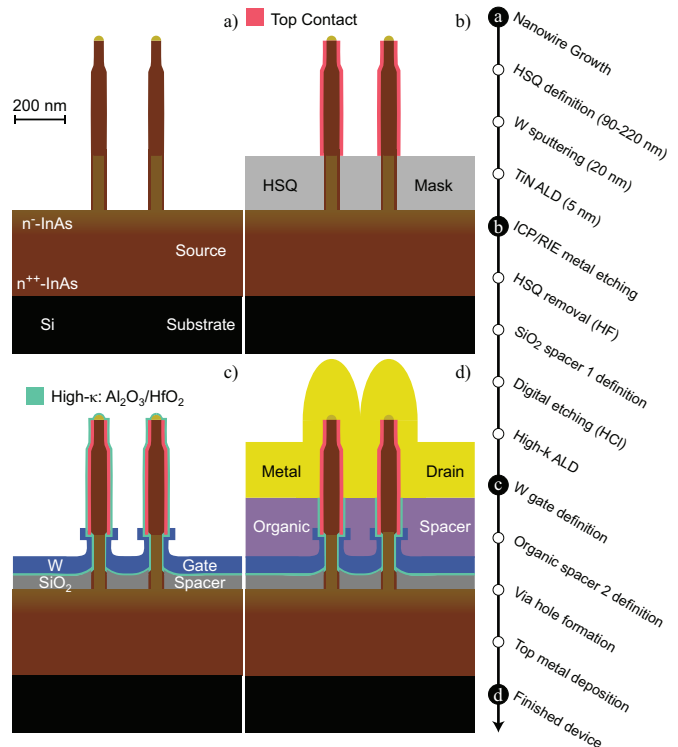


Fig. 1. Cross-sectional schematic illustrations of the most crucial steps in the self-aligned, gate-last fabrication process corresponding to the steps of the process flow chart.

## III. DEVICE FABRICATION

InAs nanowire MOSFETs are fabricated on lowly p-doped Si (111) substrates with an epitaxially grown InAs buffer layer [6]. The InAs layer serves both as a buffer layer for nanowire growth and as a low-resistive device bottom contact, avoiding transport over the InAs/Si heterojunction potential barrier [7]. The nanowires are grown using metal organic vapor-phase epitaxy (MOVPE) using the vapor-liquid-solid (VLS) method from electron-beam defined Au particles positioned in double-row arrays with 200 nm spacing. The nanowires consist of a 200 nm long undoped core segment with a diameter of 35 nm, followed by a 400 nm highly doped top segment. By increasing the group V to group III molar ratio in the second step, the highly n-doped InAs also overgrows on the undoped section, forming a 10 nm thick shell surrounding the undoped core, as illustrated in Fig. 1a.

To define the top contact, hydrogen silsesquioxane (HSQ) is applied and exposed with an electron beam at an acceleration voltage of 50 kV, where the exposure dose determines

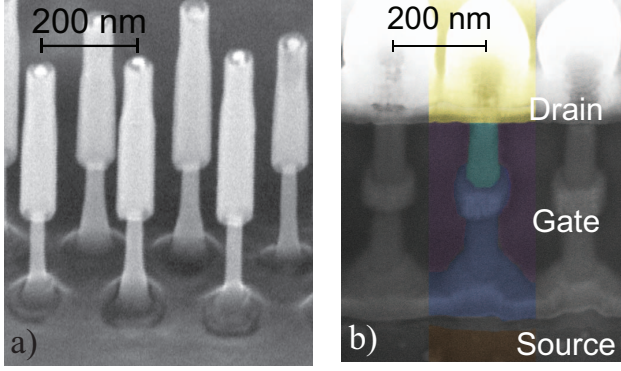


Fig. 2. Scanning electron micrographs of a) nanowires after thinning of the channel region using digital etching and b) after the complete fabrication. Both images are taken at a tilt of  $52^\circ$  from top-view.

the thickness of the film after development. The top metal contact is formed by sputtering of 20 nm W and atomic layer deposition (ALD) of 5 nm TiN. The metal layers are dry etched anisotropically, removing the planar layer keeping only the metal on the nanowire sidewalls, as illustrated in Fig. 1b. The HSQ is subsequently wet etched using HF.  $\text{SiO}_2$  is deposited using ALD followed by etch back of a spin-on resist. This resist serves as etch mask for HF wet etching of  $\text{SiO}_2$  from the nanowire sidewalls, which results in a 20-nm-thick  $\text{SiO}_2$  separation layer between gate and source. This spacer, together with the top metal, also serves as an etch mask for digital etching of the nanowires using alternating  $\text{O}_3$  oxidation for 10 min at  $50^\circ\text{C}$  and  $\text{HCl} : \text{H}_2\text{O}$  (1:10) etching for 15 s. The segment not protected by etch masks, corresponding to  $L_G$ , is ultimately determined by the exposure dose of the top metal definition, and in this case varied between 70 and 200 nm. A channel diameter of 28 nm is fabricated while keeping thicker doped regions underneath the top contact and the bottom spacer. An ALD high- $\kappa$  oxide, corresponding to an approximate EOT of 1.5 nm, consisting of a bi-layer of  $\text{Al}_2\text{O}_3$  and  $\text{HfO}_2$ , is deposited at  $300^\circ\text{C}$  and  $120^\circ\text{C}$ , respectively. This is followed by gate metal sputtering of W and definition of the gate edge using an

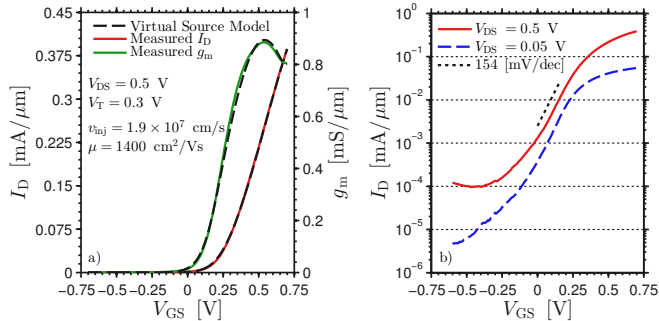


Fig. 3. Transfer characteristics with a) a linear scale and b) a logarithmic scale for a vertical InAs nanowire MOSFET consisting of 280 nanowires in parallel with a diameter of 28 nm and  $L_G$  of 190 nm. The dashed black line of a) is a fitting of a virtual source model using an injection velocity,  $v_{\text{inj}}$ , of  $1.9 \times 10^7 \text{ cm s}^{-1}$  and a mobility,  $\mu$ , of  $1400 \text{ cm}^2 \text{ V}^{-1} \text{ s}^{-1}$ .

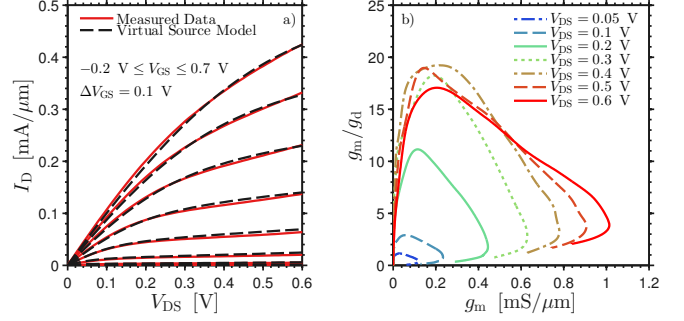


Fig. 4. a) Output characteristics for the same transistor as in Fig. 3 together with the corresponding virtual source modeling. b) Voltage gain,  $g_m/g_d$ , as a function of  $g_m$  for the same device.

etched back spin-on resist. An illustration can be seen in Fig. 1c, showing an overlapping gate on the top side and edge-to-edge alignment on the source-side. A 100 nm organic second spacer is fabricated followed by sputtering of the top metal electrode stack with the final device architecture shown in Fig. 1d. Scanning electron micrographs of the devices after the thinning of the channel region and after the complete fabrication are shown in Fig. 2a and Fig. 2b, respectively.

#### IV. RESULTS AND DISCUSSION

The transfer characteristics for a vertical InAs nanowire MOSFET with a channel diameter of 28 nm and a gate length of 190 nm can be seen in Fig. 3. A peak transconductance,  $g_{m,\text{max}}$ , of  $0.85 \text{ mS } \mu\text{m}^{-1}$ , normalized to the circumference, and a minimum subthreshold swing,  $SS$ , of  $154 \text{ mV dec}^{-1}$  is measured at  $V_{\text{DS}} = 0.5 \text{ V}$ . Furthermore, enhancement mode operation is observed with a  $V_T = 0.3 \text{ V}$ . The device characteristics are modeled using a virtual source model [8], and show good fit to measured transfer and output data, illustrated in Fig. 3a and Fig. 4a, using an injection velocity,  $v_{\text{inj}}$ , of  $1.9 \times 10^7 \text{ cm s}^{-1}$  and an electron mobility,  $\mu_e$ , of  $1400 \text{ cm}^2 \text{ V}^{-1} \text{ s}^{-1}$ . Fig. 4b shows the voltage gain,  $g_m/g_d$ , as a function of  $g_m$  and  $V_{\text{DS}}$  for the same device. The good electrostatic control provides high gain at low

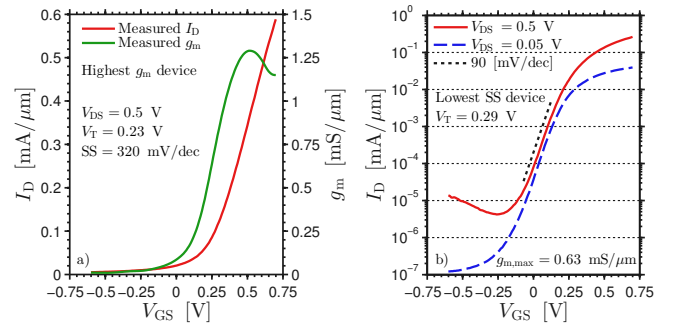


Fig. 5. Transfer characteristics for two different devices with a) being the one with the highest  $g_{m,\text{max}}$  of  $1.29 \text{ mS } \mu\text{m}^{-1}$  and b) the one with the lowest subthreshold swing of  $90 \text{ mV dec}^{-1}$ . Both transistors have a diameter of 28 nm, but have different gate lengths, with a) and b) corresponding to 130 nm and 180 nm, respectively.

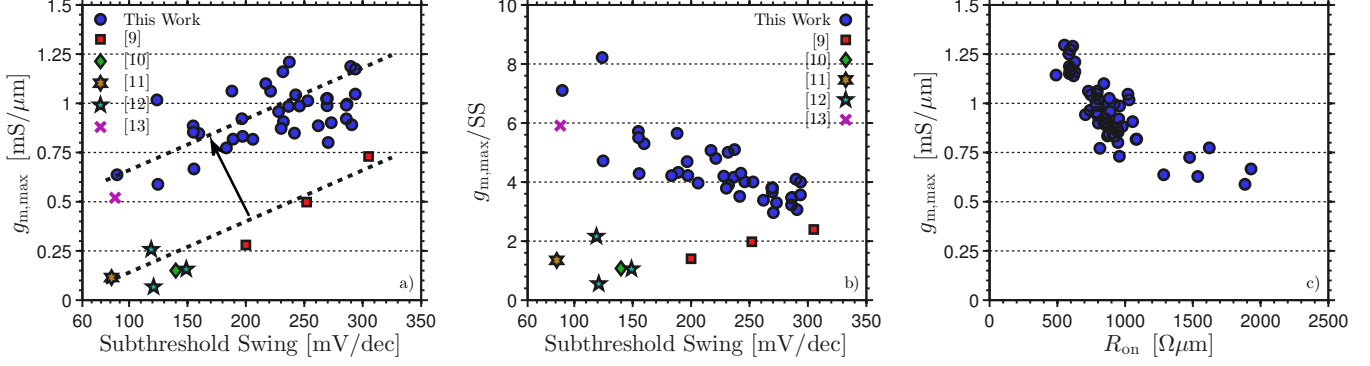


Fig. 6. a) Transconductance as a function of subthreshold swing for the fabricated devices in this work compared to other reported vertical III-V nanowire MOSFETs. Our values compare favorably to others both in terms of transconductance and subthreshold swing. b)  $Q = g_{m,\max}/SS$  as a function of  $SS$  for the same devices as a). A clear trend with increasing values for lower subthreshold swings, indicating that even higher performance can be expected with an improved gate stack. c)  $g_{m,\max}$ , extracted at  $V_{DS} = 0.5$  V, as a function of  $R_{on}$  for multiple devices fabricated in parallel. A large increase in  $g_{m,\max}$  is observed for lower  $R_{on}$ , demonstrating that the performance is limited by extrinsic series resistances. In the three graphs, data from identically fabricated devices positioned in a hexagonal geometry is included.

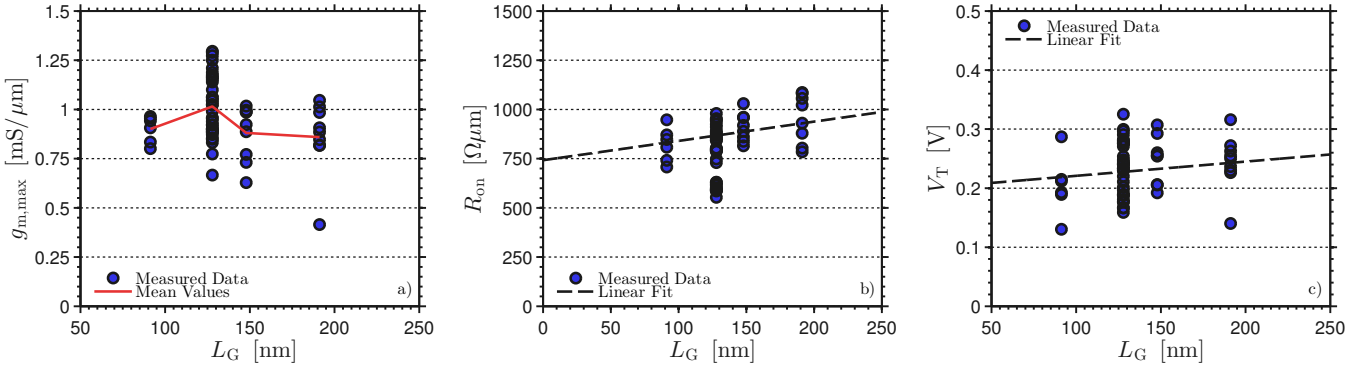


Fig. 7. a) Peak transconductance at  $V_{DS} = 0.5$  V versus gate length for devices with the same diameter fabricated in parallel. A trace representing the mean transconductance at each gate length is included. A slight increase in  $g_m$  as  $L_G$  is reduced is observed down to 120 nm. b) On-resistance as a function of gate length. A linear extrapolation to zero  $L_G$  indicates an average access resistance of about  $750 \Omega \mu\text{m}$ . c) Threshold voltage versus gate length showing a small negative shift with shorter channels and a variation, on the order of 150 mV, between devices.

gate overdrive, although it is lowered as  $g_m$  approaches  $g_{m,\max}$ , originating from series resistances on both the drain and source. The transfer characteristics for the devices with the highest  $g_{m,\max}$  and the lowest  $SS$ , corresponding to  $1.29 \text{ mS } \mu\text{m}^{-1}$  and  $90 \text{ mV dec}^{-1}$ , are shown in Fig. 5a and b, respectively. The DC performance metrics are extracted for 60 devices with varying gate lengths and compared to other vertical III-V nanowire MOSFETs [9]–[13]. Fig. 6a and b show that the fabricated devices with the self-aligned gate-last process compare favorably to other work, especially the improved  $Q = g_{m,\max}/SS$  [14] demonstrates that our fabrication method yields a good combination of on and off performance. The highest value for  $Q$  is 8.2, which is, to the authors knowledge, higher than for any previously demonstrated vertical nanowire MOSFET. Fig. 6c show  $g_{m,\max}$  plotted versus  $R_{on}$  and it indicates that  $g_m$  is limited by access resistance. From the virtual source modelling, shown in Fig. 3a, the intrinsic  $g_{m,\max}$  is estimated to  $2.2 \text{ mS } \mu\text{m}^{-1}$ .

Devices with different  $L_G$  in the range between 70 and 200 nm are fabricated by varying the first HSQ layer thick-

ness. The impact of a varying  $L_G$  is shown for  $g_{m,\max}$ ,  $R_{on}$ , and the threshold voltage,  $V_T$ , in Fig. 7a-c, respectively. A small increase in  $g_m$  as  $L_G$  is reduced can be observed, combined with a lowering of  $V_T$ . From the  $R_{on}$  dependency, an average access resistance for these devices of about  $750 \Omega \mu\text{m}$  is extracted, further indicating that the device DC performance is limited by access resistance. By comparing measurements when keeping the bottom of the nanowires grounded to top-ground measurements, it is found that the majority of the resistance is situated on the top side, probably due to high contact resistance at the W-InAs interface.

## V. CONCLUSION

In this work, we have demonstrated the highest performance in terms of  $g_{m,\max}$  and  $SS$  for any vertical nanowire MOSFET, with  $g_{m,\max}$  reaching  $1.29 \text{ mS } \mu\text{m}^{-1}$  and  $SS$  of  $90 \text{ mV dec}^{-1}$ . This performance is achieved through the use of a novel self-aligned, gate-last fabrication process on a Si-substrate. The method allows for gate length scaling as well as separate optimization of the channel region and the contact regions.

## VI. ACKNOWLEDGEMENTS

This work was supported in part by the Swedish Research Council, in part by the Knut and Alice Wallenberg Foundation, and in part by the Swedish Foundation for Strategic Research, and the European Union H2020 Program INSIGHT (Grant Agreement No. 688784).

## REFERENCES

- [1] "The international technology roadmap for semiconductors (itrs): 2012 update," Tech. Rep., 2012. [Online]. Available: <http://www.itrs.net/>
- [2] P. Caroff, M. E. Messing, B. M. Borg, K. A. Dick, K. Deppert, and L.-E. Wernersson, "Insb heterostructure nanowires: Mopve growth under extreme lattice mismatch," *Nanotechnology*, vol. 20, no. 49, p. 495606, 2009. [Online]. Available: <http://stacks.iop.org/0957-4484/20/i=49/a=495606>
- [3] D. Yakimets, G. Eneman, P. Schuddinck, T. H. Bao, M. Bardon, P. Raghavan, A. Veloso, N. Collaert, A. Mercha, D. Verkest, A. Voon-Yew Thean, and K. De Meyer, "Vertical gaafets for the ultimate cmos scaling," *Electron Devices, IEEE Transactions on*, vol. 62, no. 5, pp. 1433–1439, May 2015.
- [4] K. Jansson, E. Lind, and L.-E. Wernersson, "Performance Evaluation of III-V Nanowire Transistors," *IEEE Trans. Electron Devices*, vol. 59, no. 9, pp. 2375–2382, SEP 2012.
- [5] C. Rolland, P. Caroff, C. Coinon, X. Wallart, and R. Leturcq, "Inhomogeneous si-doping of gold-seeded inas nanowires grown by molecular beam epitaxy," *Applied Physics Letters*, vol. 102, no. 22, pp. –, 2013. [Online]. Available: <http://scitation.aip.org/content/aip/journal/apl/102/22/10.1063/1.4809576>
- [6] S. G. Ghalamestani, M. Berg, K. A. Dick, and L.-E. Wernersson, "High quality InAs and GaSb thin layers grown on Si (111)," *J. Cryst. Growth*, vol. 332, no. 1, pp. 12–16, Oct 2011.
- [7] C. Rehnstedt, T. Martensson, C. Thelander, L. Samuelson, and L.-E. Wernersson, "Vertical inas nanowire wrap gate transistors on si substrates," *Electron Devices, IEEE Transactions on*, vol. 55, no. 11, pp. 3037–3041, Nov 2008.
- [8] A. Khakifirooz, O. Nayfeh, and D. Antoniadis, "A simple semiempirical short-channel mosfet current-voltage model continuous across all regions of operation and employing only physical parameters," *Electron Devices, IEEE Transactions on*, vol. 56, no. 8, pp. 1674–1680, Aug 2009.
- [9] X. Zhao, J. Lin, C. Heidelberger, E. Fitzgerald, and J. del Alamo, "Vertical nanowire ingaas mosfets fabricated by a top-down approach," in *Electron Devices Meeting (IEDM), 2013 IEEE International*, Dec 2013, pp. 28.4.1–28.4.4.
- [10] K.-M. Persson, M. Berg, M. Borg, J. Wu, S. Johansson, J. Svensson, K. Jansson, E. Lind, and L.-E. Wernersson, "Extrinsic and intrinsic performance of vertical inas nanowire mosfets on si substrates," *Electron Devices, IEEE Transactions on*, vol. 60, no. 9, pp. 2761–2767, Sept 2013.
- [11] K. Tomioka, M. Yoshimura, and T. Fukui, "A III-V nanowire channel on silicon for high-performance vertical transistors," *Nature*, vol. 488, no. 7410, pp. 189–192, 2012.
- [12] K.-M. Persson, E. Lind, A. Dey, C. Thelander, H. Sjolund, and L.-E. Wernersson, "Low-frequency noise in vertical inas nanowire fets," *Electron Device Letters, IEEE*, vol. 31, no. 5, pp. 428–430, May 2010.
- [13] C. Thelander, L. FrobergFroberg, C. Rehnstedt, L. Samuelson, and L.-E. Wernersson, "Vertical enhancement-mode inas nanowire field-effect transistor with 50-nm wrap gate," *Electron Device Letters, IEEE*, vol. 29, no. 3, pp. 206–208, March 2008.
- [14] G. Doornbos and M. Passlack, "Benchmarking of iii-v n-mosfet maturity and feasibility for future cmos," *Electron Device Letters, IEEE*, vol. 31, no. 10, pp. 1110–1112, Oct 2010.